

Fluorescence quenching in an organic donor-acceptor dyad: A first principles study

T. Körzdörfer,^{1,a)} S. Tretiak,² and S. Kümmel¹

¹Physics Institute, University of Bayreuth, D-95440 Bayreuth, Germany

²Theoretical Division, Center for Nonlinear Studies (CNLS) and Center for Integrated Nanotechnologies (CINT), Los Alamos National Laboratory, Los Alamos, New Mexico 87545, USA

(Received 14 April 2009; accepted 9 June 2009; published online 21 July 2009)

Perylene bisimide and triphenyl diamine are prototypical organic dyes frequently used in organic solar cells and light emitting devices. Recent Förster-resonant-energy-transfer experiments on a bridged organic dyad consisting of triphenyl diamine as an energy-donor and perylene bisimide as an energy-acceptor revealed a strong fluorescence quenching on the perylene bisimide. This quenching is absent in a solution of free donors and acceptors and thus attributed to the presence of the saturated $\text{CH}_2\text{O}(\text{CH}_2)_{12}$ -bridge. We investigate the cause of the fluorescence quenching as well as the special role of the covalently bound bridge by means of time dependent density functional theory and molecular dynamics. The conformational dynamics of the bridged system leads to a charge transfer process between donor and acceptor that causes the acceptor fluorescence quenching. © 2009 American Institute of Physics. [DOI: 10.1063/1.3160666]

I. INTRODUCTION

Photoinduced transfer of electronic excitation energy and charges are among the most prominent phenomena both in biology, e.g., in photosynthesis, and in modern material science, e.g., in organic solar cells or light emitting diodes. In the past decades, considerable progress has been made in the understanding of energy and charge transfer processes. Hopes are high that a better understanding will allow one to improve the efficiency of organic photovoltaics (see Refs. 1–4 for an overview). In many investigations, especially tailored model systems based on π -conjugated organic molecules play a prominent role. Examples are molecular switches,⁵ light harvesting systems,⁶ dendrimers⁷ and self-organized polymers⁸ based on perylene dyes, *J*-aggregates,⁹ and organic donor-bridge-acceptor (DBA) systems.^{10–12}

Among the most prominent organic compounds used in these model systems, as well as in current applications are the π -conjugated dyes perylene bisimide (PTCDI) and triphenyldiamine (TPD) (see Fig. 1). PTCDI is a thermally and photochemically stable organic semiconductor that grows highly ordered thin films on different inorganic substrates and has been incorporated in a variety of electronic devices such as organic field-effect transistors¹³ or photovoltaics.¹⁴ TPD is widely used in hole transport layers of photoelectronic devices¹⁵ due to its good hole injection and mobility characteristics. Furthermore, both PTCDI and TPD show strong fluorescence in the visible range¹² and the emission spectrum of TPD overlaps with the absorption spectrum of PTCDI. Thus, TPD and PTCDI are an ideal pair to study resonant excitation energy transfer.

Following this line of thought, a DBA system consisting of TPD (D) as an energy-donor and PTCDI (A) as an energy acceptor linked by a saturated and flexible $\text{CH}_2\text{O}(\text{CH}_2)_{12}$ -

bridge (B) has recently been synthesized¹¹ and studied¹² as a model system for excitation energy transfer. Making use of time-resolved and fluorescence emission spectroscopy this study revealed an efficient photoinduced energy transfer from D to A. However, simultaneously a strong quenching of the A-fluorescence was found. As this quenching is absent in a solution of free donors and acceptors, it is obviously attributed to the presence of the saturated bridge. The aim of this manuscript is to clarify the role of the saturated bridge in the quenching process by means of time-dependent density functional theory (TDDFT) and molecular dynamics (MD).

To this end, our manuscript is organized as follows: after a short introduction to the experimental observations, we summarize the used methods in Sec. III. In Sec. IV we present and discuss our results before concluding in Sec. V.

II. THE EXPERIMENT

In the following we introduce the experimental results as far as this is necessary to follow the upcoming discussion. Details can be found in the original publication.¹² The

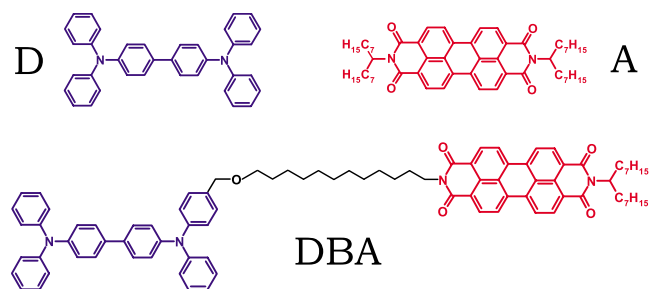


FIG. 1. The investigated materials: TPD (D): *N,N'*-Bis(3-methylphenyl)-*N,N'*-bis(phenyl)benzidine, PTCDI (A): 2,9-Bis-(1-heptyl-octyl)-anthra[2,1,9-def; 6,5,10-*d'e'f'*]-diisochinoline-1,3,8,10-tetraone, DBA molecule: 9-[12-*N*-(4-benzyloxy)-*N,N',N'*-triphenyl benzidinedodecyl]-2-(1-heptyloctyl)-anthra[2,1,9-def;6,5,10-*d'e'f'*]-diisochinoline-1,3,8,10-tetraone.

^{a)}Electronic mail: thomas.koerzdoerfer@uni-bayreuth.de.

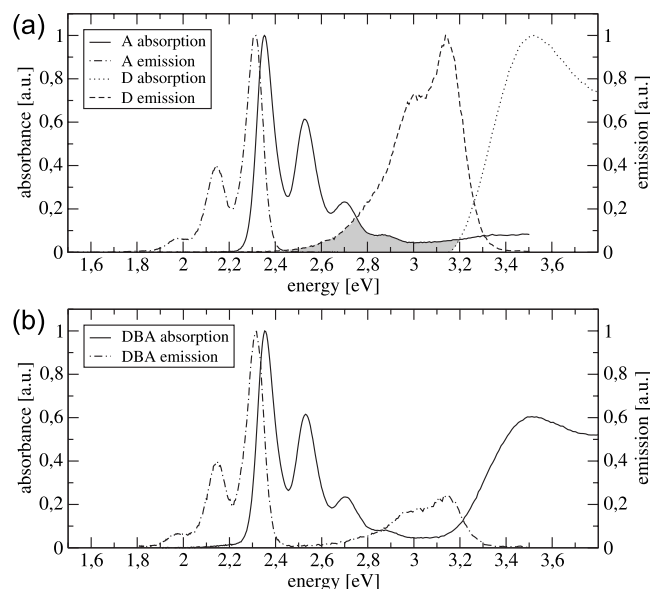


FIG. 2. (a) Absorption and emission spectra of D and A in toluene. (b) Absorption and emission spectra of DBA in toluene. The emission spectrum of DBA has been excited at 3.5 eV (Ref. 17).

system under investigation is the DBA molecule 9-[12-*N*-(4-benzyloxy)-*N,N',N'*-triphenyl benzidine-dodecyl]-2-(1-heptyloctyl)-anthra-[2,1,9-def;6,5,10-*d'e'f'*]-diisochinoline-1,3,8,10-tetraone (see Fig. 1), which we will abbreviate as DBA in the following. Initially, D and A were dissolved separately in toluene and investigated via fluorescence spectroscopy. Figure 2(a) shows the absorption and emission spectra of D and A. After chemically linking D and A with the $\text{CH}_2\text{O}(\text{CH}_2)_{12}$ -bridge and dissolving the resulting DBA in toluene the absorption spectrum shown in Fig. 2(b) is measured. In addition, Fig. 2(b) provides the emission spectrum of DBA as induced by an excitation at 3.5 eV, i.e., at the absorption energy of D. Obviously, the excitation of D is followed by an efficient excitation energy transfer to A. Thus, the resulting DBA emission spectrum appears as a superposition of the D and A emission spectra. Apart from this, the saturated bridge has only minor effects on the position of the absorption and emission energies.

The decay rates k_D and k_A of D and A, respectively, are provided in Table I. The energy transfer in DBA and in a solution of free donors and acceptors (D+A) leads to an increase in the measured decay rate k_D^{DBA} of D in DBA, i.e.,

$$k_D^{\text{DBA}} = k_D + k_{\text{ET}}. \quad (1)$$

Thus, the energy transfer rate k_{ET} can be determined by measuring k_D and k_D^{DBA} . Utilizing k_{ET} in the standard Förster-

TABLE I. Experimental fluorescence energies and decay rates of D, A, D + A (at concentrations $c_D=2.3$ mM and $c_A=6.2$ mM) and DBA in toluene as provided in Ref. 12; energies are taken at the maxima of the emission spectra; exp. k_D in DBA is on the edge of the instrument response threshold.

	E_D (eV)	k_D (1/ns)	E_A (eV)	k_A (1/ns)
D	3.1	1.18
A	2.3	0.25
D+A	3.1	1.75	2.3	0.25
DBA	3.1	>12.5	2.3	0.59

resonant-energy-transfer (FRET)-methodology, the authors of Ref. 12 derive a D-A distance in DBA that corresponds to a fully stretched conformation of the bridge.

Note that Table I reveals evidence on other electronic processes in the system. The substantial increase in the decay rate k_A^{DBA} of A in DBA as compared to free A indicates an efficient quenching process. From

$$k_A^{\text{DBA}} = k_A + k_Q, \quad (2)$$

one finds a quenching rate k_Q of 0.33 1/ns. This finding reveals the presence of an additional nonradiative decay channel in the bridged system. In contrast to the energy transfer process [see. Eq. (1)], this decay channel is absent in a solution of free donors and acceptors. Furthermore, it occurs independently of the energy transfer passage, i.e., the quenching can also be observed if one excites DBA directly at the A absorption.

A possible and frequently invoked explanation for fluorescence quenching in this type of systems is charge transfer. A charge transfer coupling between D and A could be caused either by a superexchange coupling through the saturated bridge (see e.g., Refs. 1, 2, and 16 for an overview of the superexchange formalism) or by a collapse of the bridge in solution that leads to orbital overlap of D and A. As for the former, a superexchange coupling as strong as the one observed here would be quite unusual considering the length of the $\text{CH}_2\text{O}(\text{CH}_2)_{12}$ -bridge. Our DFT calculations described below address questions of electronic coupling insofar as they give detailed insight into the electronic properties of the DBA-system. As for the latter, it must be noted that a collapse of the bridge in solution seems to contradict the findings of Ref. 12 concerning the distance between D and A. The derivation of this distance however is based on the FRET-methodology, i.e., D and A are approximated as interacting point dipoles. Higher order multipoles as well as electronic and vibrational couplings of D, B, and A are completely neglected. Depending on the particularities of the investigated system, these approximations can influence the distance-dependence of the energy-transfer rate significantly.¹⁸ Therefore, distances derived by using standard FRET-methodology can either be over- or underestimated. As a consequence, the D-A distance derived in Ref. 12 may not be trustworthy. However, if the hydrocarbon bridge folds so that D and A couple electronically, one would expect this coupling to have a significant influence on the measured DBA-spectra, e.g., similar to the situation found for the PTCDI dimer whose spectrum shows strong deviations from the monomer spectrum due to orbital overlap.¹⁹ Yet Fig. 2 demonstrates that this is not the case.

Summing up these observations one can only conclude that the information from the fluorescence spectroscopy measurements is not conclusive. A theoretical analysis can shed light on these findings. Therefore a detailed study of the role of the bridge in the observed fluorescence quenching by means of DFT, TDDFT, and MD is the aim of this manuscript.

III. METHODOLOGY

Quantum chemical calculations are performed using the linear-response TDDFT formalism as implemented in the TURBOMOLE v5.10 (Ref. 20) and GAUSSIAN03 (Ref. 21) program packages. Ground state molecular geometries of D, A, and DBA are obtained from TURBOMOLE geometry optimization²² employing an empirical dispersion correction.²³ Unless otherwise noted, all DFT and TDDFT calculations make use of the B3LYP functional²⁴ and an SVP basis set.²⁵ No symmetries are enforced. Solution effects are simulated using COSMO.^{26,27} The natural transition orbitals (NTO) approach²⁸ is used to identify and visualize electronic excitations. MD calculations are performed using the TINKER program package²⁹ and the MM3 force field.³⁰ Pre- and post-processing operations are performed with the help of VIEWMOL (Ref. 31) and VMD.³²

IV. RESULTS AND DISCUSSION

We start our computational analysis by calculating the ground-state geometrical structures and Kohn–Sham (KS) eigenvalue spectra of D and A using DFT. Unless otherwise noted, the C₇H₁₅-sidechains of A are replaced with hydrogens in all quantum chemical calculations presented in this work. Their only purpose in the experiments is to increase the solubility of A. Beyond this, an influence of the sidechains on the ground state and/or the excited state properties of A was observed neither experimentally¹² nor computationally.³³

The geometrical structures we derived agree with the ones from earlier DFT calculations for D (Ref. 34) and A.³⁵ For details on bond length and angles we therefore refer the reader to those publications.

According to Janak's theorem,³⁶ the KS eigenvalue of the highest occupied molecular orbital (HOMO) calculated with the exact density-functional equals the ionization potential (IP).³⁷ Furthermore the difference between the HOMO and the lowest unoccupied molecular orbital (LUMO) eigenvalues can be interpreted as an approximation to the experimental excitation energy.^{38,39} Although strictly speaking the latter approximation is not applicable to hybrid functionals, it is known in the literature that in practice the B3-LYP gap often yields a good approximation to the true optical gap.^{40,41} Following this line of thought, one can gain a first insight into the processes involved in the above described experiments by drawing a highly approximative but instructive one-particle picture.

We start by comparing our DFT results with cyclic voltametry experiments.¹¹ The HOMO energies of -4.90 eV for D and -5.92 eV for A agree well with the experimental IPs of -5.10 and -6.03 eV, respectively. Using the calculated LUMO-energies of -1.16 eV for D and -3.43 eV for A yields approximative excitation energies of 3.74 and 2.49 eV. They compare surprisingly well with the experimentally observed excitation energies of 3.5 and 2.35 eV, respectively.⁴² The uppermost box in Fig. 3 sketches the relative position of the HOMO- and LUMO-energies of D and A, drawing an intuitive one-particle picture of the observed processes. As indicated by the left hand sides of the two circles in Fig. 3,

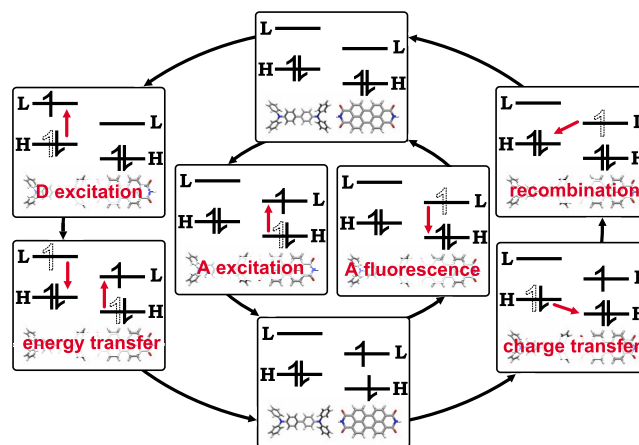


FIG. 3. Approximate one-particle picture of the observed processes in DA following optical excitation. HOMO (H) and LUMO (L) energies are positioned according to DFT results. Energy transfer, charge transfer, and charge recombination are nonradiative processes and therefore cannot be observed directly in fluorescence spectroscopy measurements.

there are two main pathways for going from a mixture of free donors and acceptors in their ground states (DA) to a configuration with an excited acceptor (DA*). While the inner circle indicates the obvious pathway, i.e., the direct excitation of DA at the acceptor absorption energy, the outer circle involves an excitation of DA at the donor absorption energy followed by a nonradiative energy transfer to the acceptor. It is important to recapture that in Ref. 12 these two pathways have been used experimentally to generate DBA* and that for both pathways an efficient quenching of the acceptor fluorescence was found. Therefore, besides the acceptor fluorescence (indicated by the inner circle on the right hand side of Fig. 3) there must exist at least one additional, nonradiative pathway going back from the photoexcited state (DA*) to the ground state (DA).

The approximative one-particle picture suggests such a nonradiative pathway. It is indicated by the outer circle on the right hand side of Fig. 3. Starting from DA*, the system undergoes a charge transfer from the HOMO of D to the HOMO of A. This charge-separated state turns into the neutral state through charge recombination. Obviously, the occurrence of this pathway requires charge transfer coupling between D and A. Contrary to the long-range energy transfer coupling which falls off as $\sim 1/r^3$,⁴³ charge transfer coupling is a short-range interaction that decays exponentially.¹ As a consequence, there is a wide range of D-A distances in which energy transfer takes place whereas charge transfer does not. Obviously, the D+A mixture investigated in Ref. 12 features such distances. However, the fluorescence quenching in DBA indicates that the inclusion of the saturated bridge introduces charge transfer coupling between D and A and thereby opens the nonradiative de-excitation pathway suggested by the outer circle in Fig. 3.

In order to test the influence of the saturated bridge on the electronic structure of DBA we now calculate the DBA ground state with DFT. We start by analyzing the DBA conformation in which the saturated bridge is completely stretched. Clearly, this constitutes an important limit, not least because the experimental results predict such a

TABLE II. Excitation energies (in eV) and oscillator strengths (in atomic units) of D, A, D+A, and DBA in stretched and folded bridge geometry. The folded bridge geometry is the MD-step 2 geometry (see Fig. 5 and discussion in the text). Corresponding NTOs are provided in Fig. 6.

A	D	D+A	DBA stretched	DBA folded
2.41(0.627)	...	2.41(0.630)	2.40(0.707)	2.41(0.581)
...	3.26(0.107)
...	3.28(0.021)
...	3.27(1.128)	3.27(1.129)	3.26(1.198)	3.31(0.967)
...	3.33(0.010)
3.55(0.056)	...	3.55(0.054)	3.53(0.037)	3.58(0.019)
...	3.61(0.035)
...	3.59(0.015)	3.59(0.014)	3.58(0.016)	3.62(0.017)

bridge-conformation.¹² The main result of our computational analysis of stretched DBA is that the influence of the saturated bridge on the geometrical and electronic structure of D and A is negligible. The bridge features a large HOMO-LUMO gap of 9.85 eV. As a consequence, it does not affect the electronic spectra of D and A in the energy range close to their HOMO and LUMO eigenvalues. The orbitals of DBA can strictly be separated into A-, B-, and D-orbitals and even for energetically close-lying D- and A-states no splitting of the KS-eigenvalues can be observed within the numerical accuracy. Thus, there is no evidence for a through-bond charge transfer coupling of D and A in the electronic ground-state of stretched DBA. Considering the length and the HOMO-LUMO gap of the saturated hydrocarbon bridge, this finding is in line with earlier works on through-bond couplings (see, e.g., Ref. 16).

Now we go over to excited-state calculations. Table II shows TDDFT excitation energies and oscillator strengths for D, A, D+A, and DBA. For free D and A one obtains strong HOMO-LUMO transitions with large oscillator strengths at 2.41 and 3.27 eV, respectively. This is in good agreement with the experimental absorption spectrum.

For the investigation of D+A, we choose the relative orientation and distance of D and A such that is consistent with the geometry of DBA in a stretched-bridge conformation. Thus, we make sure that possible differences between the stretched DBA and D+A calculations originate only from the inclusion of the bridge. As a large number of excitations with zero or almost zero oscillator strengths is introduced by the simultaneous calculation of D and A in one system, we only provide those excitation energies with oscillator strengths larger than 10^{-2} in one of the geometries. In Table II we compare energies and oscillator strengths of corresponding excitations in different systems. The good agreement of the excitation energies and oscillator strengths of stretched DBA and D+A shows that in this case the influence of the saturated bridge is clearly negligible.

After having investigated the stretched DBA-system, the close lying next step is to investigate other conformations. However, from the computational point of view finding the global minimum of DBA is challenging as the corresponding high-dimensional energy-landscape is very flat. This is a consequence of the large number of energetically inexpensive conformational changes in the bridge. We have performed

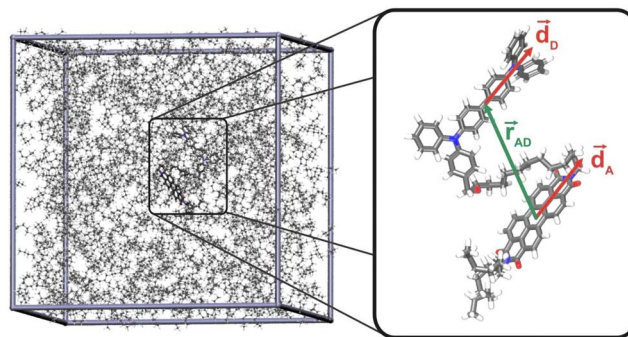


FIG. 4. MD-simulation of DBA in pentane. During the calculation, the periodic boundary box including 1170 pentane-molecules and one DBA is kept at a temperature of 298 K and a pressure of 1 atm. The time step used for the MD is 1 fs.

several steepest descent optimizations starting from different initial geometries. The local minimum in which the steepest descent relaxation ends up is strongly predetermined by the initial guess. Finding the global energy minimum would therefore require extensive simulated annealing, which is computationally costly. Yet more importantly, for further understanding of the experimental data it is not just one minimum that is of interest, but the finite-temperature conformational dynamics of DBA in solution.

Therefore, we now go over to an analysis of the conformational dynamics of DBA in solution (see Fig. 4) using MD. This step is motivated by the fact that up to this point, our results do not give any indication for a charge transfer coupling between D and A in the stretched bridge conformation of DBA. We set up MD-simulations of DBA in different solvents, assuming periodic boundary conditions, room-temperature and pressure. Solvents are taken into account explicitly. Different from the quantum chemical calculations, in the MD we explicitly take into account the C_7H_{15} -sidechains on A as they considerably influence its solubility. For the following analysis, we use the distance ($|\vec{r}_{AD}|$) between D and A, as well as the orientation factor κ^2 defined via the normalized transition dipoles (\vec{d}_D and \vec{d}_A) by

$$\kappa^2 = (\cos \Theta_T - 3 \cos \Theta_D \cos \Theta_A)^2, \quad (3)$$

where

$$\cos \Theta_T = \vec{d}_D \vec{d}_A, \quad (4)$$

$$\cos \Theta_D = \vec{d}_D \vec{r}_{AD}, \quad (5)$$

$$\cos \Theta_A = \vec{d}_A \vec{r}_{AD}, \quad (6)$$

(see also Fig. 4). A plot of the the D-A distance and κ^2 as derived from an MD-calculation of DBA in pentane is given in Fig. 5. Starting from a stretched conformation the bridge immediately starts to fold. After 2.5 ns the bridge has collapsed completely. Henceforward, D and A remain stacked at a distance of ~ 5 Å and go on executing a shear movement in the stacked position (as can be derived from the plot of κ^2). We repeated the MD-simulation using a variety of different polar (ethanole, acetone, and toluene) and unpolar (pentane, decane, dodecane, and hexadecane) solvents. In all

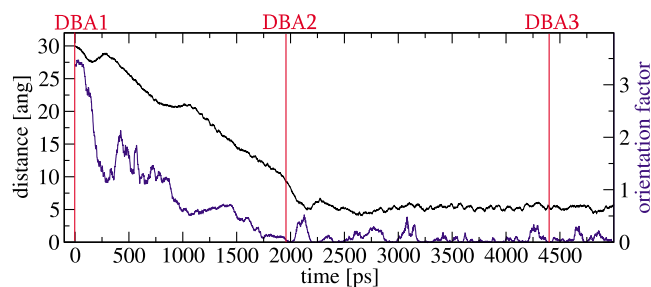


FIG. 5. Distance $|\vec{r}_{AD}|$ between D and A (see Fig. 4) and orientation factor κ^2 [see Eq. (3)] from an MD-calculation of DBA in pentane. Starting from a stretched bridge conformation, the fast folding of the bridge is followed by a shear movement of the stacked D and A.

cases we found qualitatively the same behavior. However, polarity and viscosity of the different solvents influence the average D-A distances and the time scale of the folding process. A detailed analysis of the influence of different solvents on the fluorescence depolarization and on the energy- and charge-transfer rates is thus subject of future experimental and theoretical work.

In this work however, our focus is on the charge transfer coupling between D and A. To this end, we analyze DBA for three different stages of the folding process by means of DFT and TDDFT. These stages are indicated in Fig. 5.

The first step of our MD analysis (DBA1) corresponds to the stretched bridge conformation and has been analyzed in detail above. In step 2 (DBA2) the folding process has evolved to a D-A distance of ~ 10 Å. Still, we observe no indication for electronic coupling between D and A in the ground-state calculations. In step 3 (DBA3) D and A are stacked at their final distance of ~ 5 Å. Note that the initial (DBA1) and final (DBA3) geometries of DBA are reoptimized to the next local minimum of the corresponding bridge-conformation. In contrast, the DBA2 geometry is directly taken from the MD.⁴⁴ From these calculations we find that the stacked configuration of DBA3 is energetically favored by approximately 0.55 eV as compared to DBA1 due to a π - π -stacking of D and A. The KS-orbitals at the Fermi-

level can no longer be unambiguously associated with D or A and their energies are shifted, e.g., compared to DBA1 the HOMO of A is shifted by +0.2 eV while the HOMO of D is shifted by +0.1 eV. Hence, we can clearly identify electronic coupling between D and A in DBA3 (see also discussion below). As discussed above, the electronic coupling between D and A can explain the fluorescence quenching on A. Importantly, the stacked configuration of DBA3 is thermally stable due to the large π - π -binding energy. Therefore, we expect that the soluted DBA most frequently occurs in the stacked configuration. However, one might wonder why this strong coupling cannot be observed in the experimental spectra. In search for an answer to this question we analyze the excited-state properties of DBA1-3 by means of TDDFT in the following.

A tool that allows us to visualize electronic excitations and thus facilitates the interpretation of the TDDFT results for DBA is the NTOs approach developed in Ref. 28. Given a TDDFT transition density, the NTOs provide its graphical representation in real-space by expanding the electronic excitations in the space of single KS transitions. As a result, TDDFT excitations can be characterized by single particle transitions from a hole-NTO to an electron-NTO. Thus, the NTO approach is frequently used to identify and visualize charge-transfer excitations in TDDFT.^{45,46} In our work, we use the NTOs in order to analyze the occurrence of charge-transfer excitations in the folded DBA.

Again, for DBA1 a detailed analysis of the excited state properties is provided above. As a summary of those results, the spectrum of DBA1 is basically a superposition of the excited state spectra of D and A. However, already for DBA2 the picture changes significantly. In Table II, the excitation energies and oscillator strengths of DBA2 (folded DBA) are compared to those of DBA1 (stretched DBA) and D+A. Obviously, a number of “new” excitations with nonvanishing oscillator strengths appear. The analysis of these excitations with the help of NTOs (as provided for one example in Fig. 6) reveals that these new excitations have charge-transfer

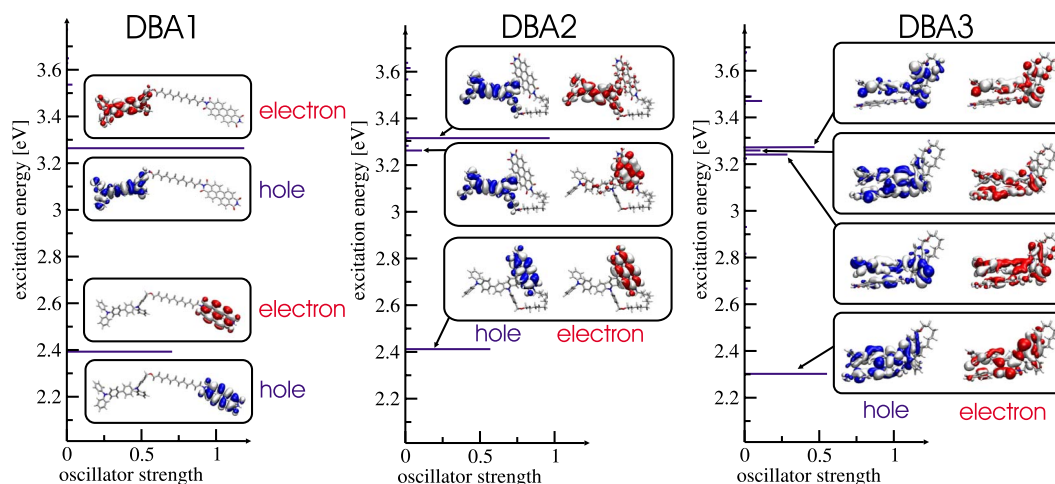


FIG. 6. TDDFT excitation spectra (see also Table II) and NTO of DBA at three stages of the MD (see Fig. 5). While in the stretched bridge conformation only pure D- and A-states occur, the folding introduces charge-transfer states. In the stacked position, a clear separation of D- and A-excitations from charge-transfer excitations is no longer possible.

character, i.e., hole- and electron-NTO are located on different parts of the DBA-molecule with some nonvanishing orbital overlap.

It is well known that local and semilocal functionals typically do not predict charge-transfer excitation correctly.⁴⁷ Although B3LYP has been shown to yield reasonable results for some charge-transfer excitations,⁴⁵ one cannot expect it to be generally accurate. This expectation is strengthened by the observation that the excitation energies of the new excitations in DBA2 vary by several eV when tuning the fraction of exact exchange in the used functional.⁴⁸ However, the purpose of our study is not to predict the energies of the charge-transfer excitations accurately—for our purposes it is enough to establish that charge transfer excitations appear. This is established without doubt by our calculations. For a detailed discussion of the charge-transfer excitation problem in TDDFT and how to deal with it we refer the reader to the pertinent literature.^{47,49}

Coming to DBA3, the excitation spectrum still shows major excitations at the original D and A excitation energies. However, the NTO-analysis reveals that the nature of these excitations has changed significantly. Obviously, a clear separation of D and A excitations is no longer possible in DBA3. Moreover, new excitations appear at the excitation energy of D. The corresponding NTOs allow for the interpretation that these are excitations of the newly formed D-A complex.

At this point, one might wonder whether the above mentioned problem of commonly used density functionals in predicting long-range charge-transfer excitations does affect the energy of those new excitations. Note however that it is not possible to distinguish clearly between charge-transfer and noncharge-transfer excitations in DBA3, as one can see from the NTOs shown in Fig. 6. This is due to the strong electronic coupling between D and A that has already been observed in the ground-state calculations. Moreover, in DBA3 the D-A distance and thus the importance of the correct description of long-range charge-transfer excitations of the used density functional is significantly reduced as compared to DBA2. As a consequence, it is reasonable to assume that long-range charge transfer does not play a prominent role in our calculations on DBA3. In order to test the above reasoning we repeated the excited state calculations on DBA3 with a number of functionals that employ different fractions of exact exchange. Different from DBA2 and different from what would be expected for long-range charge-transfer excitations, here the fraction of exact exchange has only a minor effect on the new excitations of the DA complex.⁵⁰ Thus our results are not affected significantly by the long-range charge-transfer problem of commonly used functionals.

Note also that although the nature of the excitations shown in Fig. 6 changes drastically when going from DBA1 to DBA3, the shift of the excitation energies is surprisingly small. Considering a vibrational broadening of the experimental spectra of 0.1 eV and a computational accuracy of our approach of approximately the same magnitude, this shift of the excitation energies is negligible. This explains why the

π - π -stacking of D and A cannot be observed directly in the absorption spectra. However, it becomes apparent in the A-fluorescence quenching in DBA.

The results of the above TDDFT analysis of DBA3 allow for an experimental verification of our findings. In case DBA3 *de facto* constitutes the most frequent configuration of DBA in solution, one should be able to find more than one excitation in the immediate energetic vicinity of the D excitation energy. Indeed our calculations indicate that one might not be able to distinguish between these excitations in the absorption spectrum due to vibrational broadening. However, one should be able to find several decay rates at the D-emission energy in the fluorescence spectra. From an experimental point of view this poses a challenge as the efficient energy transfer in DBA strongly shortens the lifetimes (decay rates are increased) of the D fluorescence. For these reasons, k_D^{DBA} could not be determined exactly in Ref. 12 as the corresponding lifetime was shorter than the instrument response function of 80 ps. However, recent studies of DBA employing more involved experimental techniques⁵¹ support the notion of multiple excitation energies in the frequency range of the donor emission.

At this point, it is important to make clear that our verification of the electronic coupling between D and A is a qualitative and not a quantitative one. Therefore, we cannot predict quenching rates or efficiencies. A number of *ab initio* approaches for the calculation of charge transfer rates via Marcus theory⁵² can be found in the literature.⁵³⁻⁵⁵ However, these approaches are computationally demanding and yield charge-transfer coupling elements only for one specific distance, configuration and relative orientation of the donor and acceptor molecules. It is also known that the electronic coupling is extremely sensitive to distance, relative orientation and displacement of donor and acceptor.^{3,4} In order to use these methods for predicting the experimentally observed quenching rates in our case, we therefore would have to do this type of calculation for every single time step of the MD-simulation. Clearly, this is not an option.

V. CONCLUSION

In this work, we have analyzed the role of the saturated $\text{CH}_2\text{O}(\text{CH}_2)_{12}$ -bridge in the fluorescence quenching mechanism in a DBA system that has recently been investigated experimentally. Using TDDFT and comparing calculations for a mixture of free donors and acceptors to those for the bridged DBA molecule in stretched conformation, we were able to show that the large HOMO-LUMO-gap of the saturated bridge keeps the electronic spectra of D and A completely separate. Thus, the direct influence of the bridge on the ground- and excited-state spectra of D and A is negligible. However, MD-simulations of DBA in different solvents revealed that it is the mechanical influence of the bridge that causes the acceptor-fluorescence quenching. The bridge folds in solution so that donor and acceptor stack at a distance of ~ 5 Å, which is typical for π - π stacks. In this configuration, the orbitals of donor and acceptor overlap and their spectra are electronically coupled. This coupling opens up a nonradiative de-excitation pathway including charge

transfer and recombination. As a consequence, the A-fluorescence is quenched efficiently. TDDFT calculations on the stacked DBA revealed that the electronic coupling of D and A cannot be directly observed in the absorption spectrum due to a surprisingly small shift in the excitation energies. However, the coupling leads to a multiexponential decay of the DBA-fluorescence at the donor-emission energy. This finding is in agreement with recent experimental studies.

ACKNOWLEDGMENTS

T.K. and S.K. thank C. Hofmann, P. Bauer, M. Thelakktat, and J. Köhler for stimulating discussions on the topic and for providing experimental data. T.K. acknowledges the hospitality of the Los Alamos National Laboratory. Los Alamos National Laboratory is operated by Los Alamos National Security, LLC, for the National Nuclear Security Administration of the U.S. Department of Energy under Contract No. DE-AC52-06NA25396. T.K. thanks S. Kilina, E. Badaeva, and S. Difley for fruitful discussions on charge transfer and for their help in setting up the molecular dynamics simulations. S.K. and T.K. are grateful for support from the ENB program "Macromolecular Science." T.K. gratefully acknowledges support by the Studienstiftung des deutschen Volkes.

- ¹M. Newton, *Chem. Rev. (Washington, D.C.)* **91**, 767 (1991).
- ²S. Speiser, *Chem. Rev. (Washington, D.C.)* **96**, 1953 (1996).
- ³J.-L. Brédas, D. Beljonne, V. Coropceanu, and J. Cornil, *Chem. Rev. (Washington, D.C.)* **104**, 4971 (2004).
- ⁴V. Coropceanu, J. Cornil, D. A. da Silva Filho, Y. Olivier, R. Silbey, and J.-L. Brédas, *Chem. Rev. (Washington, D.C.)* **107**, 926 (2007).
- ⁵I. B. Ramsteiner, A. Hartschuh, and H. Port, *Chem. Phys. Lett.* **343**, 83 (2001); *Molecular Switches*, edited by B. L. Feringa (Wiley-VCH, Weinheim, 2001); M. W. Holman, P. Yan, K.-C. Ching, R. Liu, F. I. Ishak, and D. M. Adams, *Chem. Phys. Lett.* **413**, 501 (2005).
- ⁶*Advances in Photosynthesis and Respiration, Light-Harvesting Antennas in Photosynthesis*, edited by B. R. Green and W. W. Parson (Kluwer, Dordrecht, 2003), Vol. 13.
- ⁷T. Christ, F. Kulzer, T. Weil, K. Müllen, and T. Basché, *Chem. Phys. Lett.* **372**, 878 (2003); P. Tinnefeld, K. D. Weston, T. Vösch, M. Cotlet, T. Weil, J. Hofkens, K. Müllen, F. C. de Schryver, and M. Sauer, *J. Am. Chem. Soc.* **124**, 14310 (2002).
- ⁸U. Anton and K. Müllen, *Macromolecules* **26**, 1248 (1993); E. E. Neuteboom, S. C. J. Meskers, E. W. Meijer, and R. A. J. Janssen, *Macromol. Chem. Phys.* **205**, 217 (2004).
- ⁹H. Fidler, J. Knoester, and D. A. Wiersma, *J. Chem. Phys.* **95**, 7880 (1991); E. Lang, A. Sorokin, M. Drechsler, Y. V. Malyukin, and J. Köhler, *Nano Lett.* **5**, 2635 (2005).
- ¹⁰W. B. Davis, W. A. Svec, M. A. Ratner, and M. R. Wasielewski, *Nature (London)* **396**, 60 (1998); C. G. Hübner, V. Ksenofontov, F. Nolde, K. Müllen, and T. Basché, *J. Chem. Phys.* **120**, 10867 (2004); T. D. M. Bell, A. Stefan, S. Masuo, T. Vösch, M. Lor, M. Cotlet, J. Hofkens, S. Bernhard, K. Müllen, M. van der Auweraer, J. W. Verhoeven, and F. C. De Schryver, *ChemPhysChem* **6**, 942 (2005); G. Duvanel, N. Banerji, and E. Vauthey, *J. Phys. Chem. A* **111**, 5361 (2007); C. Curutchet, B. Mennucci, G. D. Scholes, and D. Beljonne, *J. Phys. Chem. B* **112**, 3759 (2008).
- ¹¹P. Bauer, H. Wietasch, S. M. Lindner, and M. Thelakktat, *Chem. Mater.* **19**, 88 (2007).
- ¹²Ch. Scharf, K. Peter, P. Bauer, Ch. Jung, M. Thelakktat, and J. Köhler, *Chem. Phys.* **328**, 403 (2006).
- ¹³G. Horowitz, F. Kouki, P. Spearman, D. Fichou, C. Noguez, X. Pan, and F. Garnier, *Adv. Mater. Weinheim, Ger.* **8**, 242 (1996); P. R. L. Malenfant, C. D. Dimitrakopoulos, J. D. Gelorme, L. L. Kosbar, T. O. Graham, A. Curioni, and W. Andreoni, *Appl. Phys. Lett.* **80**, 2517 (2002).
- ¹⁴C. W. Tang, *Appl. Phys. Lett.* **48**, 183 (1986); L. Schmidt-Mende, A. Fechtenkotter, K. Müllen, E. Moons, R. H. Friend, and J. D. MacKenzie, *Science* **293**, 1119 (2001).
- ¹⁵V. Bulović, G. Gu, P. E. Burrows, S. R. Forrest, and M. E. Thompson, *Nature (London)* **380**, 29 (1996); N. Tamoto, C. Adachi, and K. Nagai, *Chem. Mater.* **9**, 1077 (1997); E. Bellmann, S. E. Shaheen, R. H. Grubbs, S. R. Marder, B. Kippelen, and N. Peyghambarian, *ibid.* **11**, 399 (1999); Y. Shirota, *J. Mater. Chem.* **15**, 75 (2005).
- ¹⁶K. D. Jordan and M. N. Paddon-Row, *Chem. Rev. (Washington, D.C.)* **92**, 395 (1992).
- ¹⁷Experimental spectra supplied by Christiane Hofmann; also see Ref. 12.
- ¹⁸B. P. Krueger, G. D. Scholes, and G. R. Fleming, *J. Phys. Chem. B* **102**, 5378 (1998); D. Beljonne, J. Cornil, R. Silbey, P. Millie, and J.-L. Brédas, *J. Chem. Phys.* **112**, 4749 (2000); D. Beljonne, G. Pourtois, C. Silva, E. Hennebicq, L. M. Herz, R. H. Friend, G. D. Scholes, S. Setayesh, K. Müllen, and J. L. Brédas, *Proc. Natl. Acad. Sci. U.S.A.* **99**, 10982 (2002); G. D. Scholes, *Annu. Rev. Phys. Chem.* **54**, 57 (2003); S. Jang, M. D. Newton, and R. J. Silbey, *Phys. Rev. Lett.* **92**, 218301 (2004); H. Wiesenhofer, D. Beljonne, G. D. Scholes, E. Hennebicq, J.-L. Brédas, and E. Zojer, *Adv. Funct. Mater.* **15**, 155 (2005); M. E. Madjet, A. Abdurahman, and T. Renger, *J. Phys. Chem. B* **110**, 17268 (2006).
- ¹⁹A. E. Clark, C. Qin, and A. D. Q. Li, *J. Am. Chem. Soc.* **129**, 7586 (2007).
- ²⁰R. Ahlrichs, M. Bär, M. Häser, H. Horn, and C. Kölmel, *Chem. Phys. Lett.* **162**, 165 (1989); F. Furche and D. Rappoport, in *Computational Photochemistry*, edited by M. Olivucci (Elsevier, Amsterdam, 2005), Vol. 16, Chap. III.
- ²¹M. J. Frisch, G. W. Trucks, H. B. Schlegel *et al.*, Gaussian 03 (Revision D.02), Gaussian, Inc., Wallingford CT (2004).
- ²²O. Treutler and R. Ahlrichs, *J. Chem. Phys.* **102**, 346 (1995).
- ²³S. Grimme, *J. Comput. Chem.* **25**, 1463 (2004); **27**, 1787 (2006).
- ²⁴P. J. Stevens, J. F. Devlin, C. F. Chabalowski, and M. J. Frisch, *J. Phys. Chem.* **98**, 11623 (1994).
- ²⁵A. Schäfer, H. Horn, and R. Ahlrichs, *J. Chem. Phys.* **97**, 2571 (1992).
- ²⁶A. Klamt and G. Schüürmann, *J. Chem. Soc. Perkin Trans. 2* **1993**, 799.
- ²⁷COSMO is used in all calculations of geometries and excited state energies. Unless otherwise noted we used a permittivity of $\epsilon=2.0$ for all calculations. This corresponds to the permittivity of dodecane and is close to the permittivity of toluene ($\epsilon=2.4$) at room temperature, both being solvents primarily used in the experiment of Ref. 12. Note, that in the calculation of the natural transition orbitals (however, not in the energies) solution effects are neglected.
- ²⁸R. L. Martin, *J. Chem. Phys.* **118**, 4775 (2003).
- ²⁹P. Ren and J. W. Ponder, *J. Phys. Chem. B* **107**, 5933 (2003).
- ³⁰N. L. Allinger, Y. H. Yuh, and J.-H. Lii, *J. Am. Chem. Soc.* **111**, 8551 (1989); J.-H. Lii and N. L. Allinger, *ibid.* **111**, 8566 (1989); J.-H. Lii and N. L. Allinger, *ibid.* **111**, 8576 (1989).
- ³¹J. R. Hill, VIEWMOL Program, Version 2.4, 2003.
- ³²W. Humphrey, A. Dalke, and K. Schulten, *J. Mol. Graphics* **14**, 33 (1996).
- ³³For all calculations on PTCDI, we checked the influence of the sidechains on the geometrical structure, the KS-eigenvalues and TDDFT excitation spectra in the relevant energetical range.
- ³⁴M. Malagoli and J.-L. Brédas, *Chem. Phys. Lett.* **327**, 13 (2000).
- ³⁵F. Pichierri, *J. Mol. Struct.* **686**, 57 (2004).
- ³⁶J. F. Janak, *Phys. Rev. B* **18**, 7165 (1978).
- ³⁷M. Levy, J. P. Perdew, and V. Sahni, *Phys. Rev. A* **30**, 2745 (1984).
- ³⁸M. Levy, *Phys. Rev. A* **52**, R4313 (1995).
- ³⁹A. Görling, *Phys. Rev. A* **54**, 3912 (1996).
- ⁴⁰U. Salzner, J. B. Lagowski, P. G. Pickup, and R. A. Poirier, *J. Comput. Chem.* **18**, 1943 (1997).
- ⁴¹For a detailed discussion of the band-gap problem for hybrids, see, e.g., S. Kümmel and L. Kronik, *Rev. Mod. Phys.* **80**, 3 (2008).
- ⁴²Experimental excitation energies taken at the maxima of the absorption spectrum.
- ⁴³Th. Förster, *Ann. Phys.* **437**, 55 (1948).
- ⁴⁴Reoptimization of the DBA2 geometry using a dispersion correction as provided in Ref. 23 leads to a collapse of the bridge with a final D-A distance of approximately 5 Å. Note that this corresponds to the mean D-A distance found in the MD and thus supports the MD results. Note further that the dispersion correction has only minor effects on the geometry of DBA1 and DBA3.
- ⁴⁵R. J. Magyar and S. Tretiak, *J. Chem. Theory Comput.* **3**, 976 (2007).
- ⁴⁶C. Wu, S. Tretiak, and V. Y. Chernyak, *Chem. Phys. Lett.* **433**, 305 (2007); E. Badaeva and S. Tretiak, *ibid.* **450**, 322 (2008).
- ⁴⁷M. E. Casida, F. Gutierrez, J. Guan, F.-X. Gadea, D. Salahub, and J.-P.

- Daudey, *J. Chem. Phys.* **113**, 7062 (2000); D. Tozer, *ibid.* **119**, 12697 (2003); N. T. Maitra, *ibid.* **122**, 234104 (2005); J. Neugebauer, O. Gritsenko, and E. J. Baerends, *ibid.* **124**, 214102 (2006).
- ⁴⁸We calculated the excitation spectrum of DBA2 using time-dependent Hartree-Fock (TDHF) and functionals using 50% (BHandHLYP), 20% (B3LYP), and no Hartree-Fock exchange (PBE). While the HOMO-LUMO excitations of D and A varied by up to 0.4 eV, the charge-transfer excitations were generally shifted by several eV.
- ⁴⁹A. Dreuw and M. Head-Gordon, *Chem. Rev. (Washington, D.C.)* **105**, 4009 (2005).
- ⁵⁰We calculated the excitation spectrum of DBA3 using TDHF, BHandHLYP, B3LYP, and PBE. The shift of all relevant excitations varied up to 0.4 eV. Thus the long-range charge transfer problem of commonly used functionals does not affect our results on DBA3.
- ⁵¹C. Hofmann and J. Köhler, private communication (2009).
- ⁵²R. A. Marcus, *J. Chem. Phys.* **24**, 966 (1956); *Rev. Mod. Phys.* **65**, 599 (1993).
- ⁵³G. Pourtois, D. Beljonne, J. Cornil, M. A. Ratner, and J.-L. Brédas, *J. Am. Chem. Soc.* **124**, 4436 (2002); V. Lemaire, M. Steel, D. Beljonne, J.-L. Brédas, and J. Cornil, *ibid.* **127**, 6077 (2005).
- ⁵⁴T. Kawatsu, V. Coropceanu, A. Ye, and J.-L. Brédas, *J. Phys. Chem. C* **112**, 3429 (2008).
- ⁵⁵Q. Wu and T. van Voorhis, *J. Chem. Phys.* **125**, 164105 (2006).